

experimental, is required. Our own optical studies are being extended to shorter wavelengths to determine if the 25-eV loss can be obtained from optical data. Efforts are also being made to extend the numerical analysis of reflectance data to anisotropic media.

#### ACKNOWLEDGMENTS

The authors acknowledge the valuable assistance received from F. L. Carlsen, Jr., of the Metals and Ceram-

ics Division of the Oak Ridge National Laboratory. Mr. Carlsen furnished the graphite and coordinated all the structural measurements presented in this paper. We acknowledge J. O. Stiegler who made the electron diffraction and transmission measurements, C. J. Sparks the orientation measurements, and R. M. Steele and F. L. Carlsen, Jr., for the x-ray diffraction measurements. We thank E. T. Arakawa for helpful discussion during the entire experiment.

PHYSICAL REVIEW

VOLUME 137, NUMBER 2A

18 JANUARY 1965

## Auger-Type Electron Ejection from the (111) Face of Nickel by Slow He<sup>+</sup>, Ne<sup>+</sup>, and Ar<sup>+</sup> Ions

Y. TAKEISHI\* AND H. D. HAGSTRUM

*Bell Telephone Laboratories, Murray Hill, New Jersey*

(Received 26 August 1964)

Experimental results concerning electron ejection from the atomically clean (111) face of nickel by singly charged ions of He, Ne, and Ar are reported. Total yield and kinetic-energy distribution of ejected electrons were measured as functions of ion energy in the range 4 to 100 eV. Revised experimental procedures have made it possible to extend the range of useful incident ion energies from the previous 10-eV lower limit down to 4 eV. Significant differences in the electron energy distributions are observed for ions whose energies differ by as little as 1 eV. The measured electron energy distributions were found to be markedly different from those observed for silicon and germanium as well as for tungsten and molybdenum. This is the result of differing state densities in the filled bands of these materials. The basic features of the results are only briefly discussed, since more extensive interpretive material will be subsequently reported. Data demonstrating the cleanness of the surface and the effects of adsorption of oxygen, carbon monoxide, and hydrogen are also presented.

### I. INTRODUCTION

**A**UGER-TYPE electron ejection from clean surfaces of elemental semiconductors (silicon and germanium) as well as polycrystalline refractory metals (tungsten and molybdenum) by noble gas ions in the kinetic energy range 10 to 1000 eV has been studied and reported on previously.<sup>1,2</sup> In this paper we report the results of an experimental study of the electron ejection from the (111) face of monocrystalline nickel by He<sup>+</sup>, Ne<sup>+</sup>, and Ar<sup>+</sup> ions of incident kinetic energies  $K$  in the range 4 to 100 eV.

It has been well established that the principal electronic interaction of noble gas ions with solid surfaces in this kinetic energy range is of an Auger type. The ions are neutralized in a process (Auger neutralization) involving two electrons from the highest lying filled band in the solid. One electron tunnels into the ground state of the atom releasing energy to a second electron in the solid which becomes a fast internal secondary. Some of these latter electrons may cross the surface

barrier and are detectable outside. The observed kinetic energy distributions from clean surfaces of those materials studied so far have been accounted for in terms of this mechanism with assumed functions for the state density in the filled band and relative transition probability through the band.<sup>1,2</sup> Work on polycrystalline tungsten using noble gas and other ions has recently been reported by Propst and Lüscher.<sup>3</sup>

One of our current reasons for studying Auger electron ejection is to look into the possibility of extracting at least the coarse features of the state density near the top of the filled band of the solid from the observed electron kinetic energy distribution. The transition metals are of particular interest in this regard, and nickel is one of the best of these with which to experiment since good quality single crystals are now available and the surface structures have been extensively studied by low-energy electron diffraction.<sup>4,5</sup> Thus our primary interest in the present study has been to observe the energy distribution of ejected electrons from the clean surface

\* Present address: Central Research Laboratory, Toshiba Electric Company, Kawasaki, Japan.

<sup>1</sup> H. D. Hagstrum, Phys. Rev. **119**, 940 (1960), **122**, 83 (1961), Si and Ge.

<sup>2</sup> H. D. Hagstrum, Phys. Rev. **96**, 325 (1954), **104**, 317 (1956), **96**, 336 (1954), W; **104**, 672 (1956), Mo.

<sup>3</sup> F. M. Propst and E. Lüscher, Phys. Rev. **132**, 1037 (1963).

<sup>4</sup> L. H. Germer, A. U. Mac Rae, and C. D. Hartman, J. Appl. Phys. **32**, 2432 (1961); H. E. Farnsworth and H. H. Madden, Jr., J. Appl. Phys. **32**, 1933 (1961); L. H. Germer and A. U. Mac Rae, *ibid.* **33**, 2923 (1962).

<sup>5</sup> A. U. Mac Rae, Surface Science **1**, 319 (1964).

of Ni(111). Significant improvements of the measurements of total electron yield  $\gamma_i$  and electron energy distribution  $N_0(E)$ , have been made. The range of useful incident ion energy  $K$  has been extended from the previous 10 eV lower limit down to 4 eV and it is now feasible to measure for ion kinetic energies that differ by as little as 1 eV.

We limit ourselves in this paper to a report of the experimental aspects and results of our study on the (111) face of Ni. Experimental conditions and a brief résumé of our improved experimental techniques are presented in Sec. II, the results of the measurements of  $\gamma_i$  and  $N_0(E)$  from the clean surface in Sec. III, and results concerning the cleanness of the surface and the effects of adsorption of  $O_2$ ,  $CO$ , and  $H_2$  in Sec. IV. Use of the data in an investigation into the nature of the physical broadenings of the ejection process and in the extraction of the state density function of nickel will be made in other publications.<sup>6</sup> Since details of the apparatus and of the improved experimental procedures used in the measurements will also be published elsewhere<sup>7</sup> these are only briefly summarized in the next section.

## II. APPARATUS AND EXPERIMENTAL CONDITIONS

The apparatus used in this work is new but its principal features are essentially like those of apparatus reported previously.<sup>1,8,9</sup> The electrode arrangements are much like those of Fig. 1 of the first reference in footnote 1. The electrode assembly is mounted in a stainless steel envelope having in its base an exhaustion port, electrical lead-throughs and a gas-inlet tube which is connected internally directly to the ionization chamber. The top section of the envelope may be disconnected at a 9-in. copper-gasketed flange exposing the electrode assembly in convenient fashion for access to the source filament and target.

The particular improvements in experimental procedures are (1) modification of the mode of operation of the ion lenses, (2) stabilization of the ion-beam current to the target during a sweep of retarding potential between the target and the spherical electron collector, and (3) direct recording of the energy distribution of ejected electrons by differentiation of the sphere current in the retarding region under conditions of constant ion beam. The most important feature of the new mode of operation of the ion lenses is that the strengths of the lenses immediately preceding the target are varied proportionally to the retarding voltage  $V_{ST}$  between target  $T$  and collector  $S$ . This enables us to reduce the lower limit of useful ion energies down to 4 eV. The ion-beam current is held constant by the use

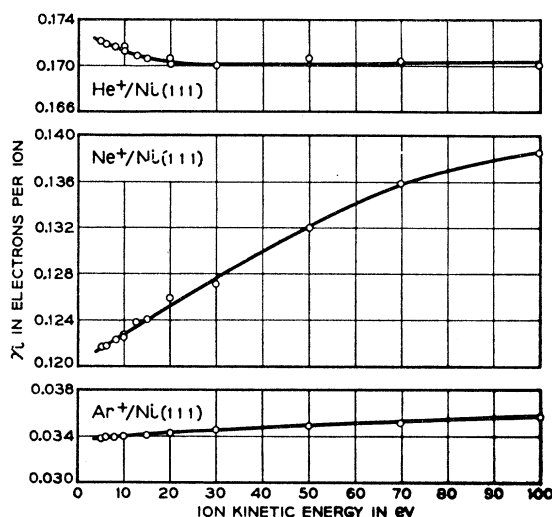


FIG. 1. Plots of total electron yield  $\gamma_i$  as a function of kinetic energy  $K$  for  $He^+$ ,  $Ne^+$ , and  $Ar^+$  ions incident on the atomically clean (111) face of nickel.

of a negative feedback loop which operates by varying the electron beam energy in the ion source making use of the variation of the ionization efficiency with bombarding electron energy. It has been held constant to within 0.2% change during a sweep of the retarding potential from  $-1$  to  $+20$  V. The kinetic energy distribution of ejected electrons is the differential of the electron current to the sphere with respect to the voltage  $V_{ST}$  in the retarding region at constant incoming ion-beam current. The voltage  $V_{ST}$  is supplied as the time integral of a constant voltage. Calculation of the ion current from signals proportional to the target and the sphere currents, differential of the sphere current, and production of the ramp voltage are all done by analog means using operational amplifiers.

The nickel target was cut from single-crystal material of high purity (99.999%) in a rectangular form, 6.3 mm wide and 10 mm long, and was polished to a thickness of 0.27 mm. The polished surface was parallel to a (111) face to about a minute. No appreciable strain was detected in Laue patterns by x-ray diffraction over all parts of the surface. Carbon-free tungsten wires of 0.75 mm diam were welded to the target and clamped to molybdenum legs. At one end of the target, a Pt-PtRh thermocouple was attached for temperature measurement. Before installation into the tube, the target was etched by an electrochemical polishing method using a mixture of 3 parts glacial acetic and 1 part perchloric acids.<sup>5,10</sup> Evacuation procedure and the vacuum conditions achieved were similar to those reported in earlier work.<sup>8</sup> The background pressure during the measurements was  $\sim 8 \times 10^{-10}$  Torr, equivalent  $N_2$  pressure, determined before the noble gas was admitted. The

<sup>6</sup> H. D. Hagstrum and Y. Takeishi (to be published).

<sup>7</sup> H. D. Hagstrum, D. D. Pretzer, and Y. Takeishi (to be published).

<sup>8</sup> H. D. Hagstrum, Rev. Sci. Instr. **24**, 1122 (1953).

<sup>9</sup> H. D. Hagstrum, Phys. Rev. **104**, 1516 (1956).

<sup>10</sup> L. H. Germer, A. U. Mac Rae, and C. D. Hartman, J. Appl. Phys. **32**, 2432 (1961).

sputtering procedure was similar to that used for the semiconductor experiments.<sup>1</sup> A current of 100-eV Ne<sup>+</sup> ions of several mA was drawn to the target from the plasma of an arc discharge in Ne between a filament behind the target and the electron collecting sphere. From the published sputtering yield of 0.22 Ni atom per 100-eV Ne<sup>+</sup> ion,<sup>11</sup> a sputtering rate of about 0.5 layer sec<sup>-1</sup> mA<sup>-1</sup> cm<sup>-2</sup> was calculated for the present experimental conditions. The sputtering was performed several times during the course of the experiment and about 50 to 100 monolayers were removed from the surface of the target at each sputtering. Each sputtering was followed by annealing for about one minute at a temperature generally near 900°K. Longer annealing was also tried. The target was always flashed to a temperature near 720°K for 15 sec immediately prior to taking the clean surface data. The cleanness of the surface was carefully confirmed by various means as discussed in Sec. IV. Thus, all data shown in the following section are believed to be for the Ni(111) face, atomically clean to within a fraction of a percent of monolayer coverage by residual gases.

Total electron yield  $\gamma_i$  in electrons per incident ion was measured as the quantity  $\rho = I_S / (I_T + I_S)$  at a slightly negative value of the voltage  $V_{ST}$ .  $I_T$  and  $I_S$  are the target and the sphere current, respectively, and both are recorded 15 or 20 sec after the target flash by digital means. The total yield data for Ni are given

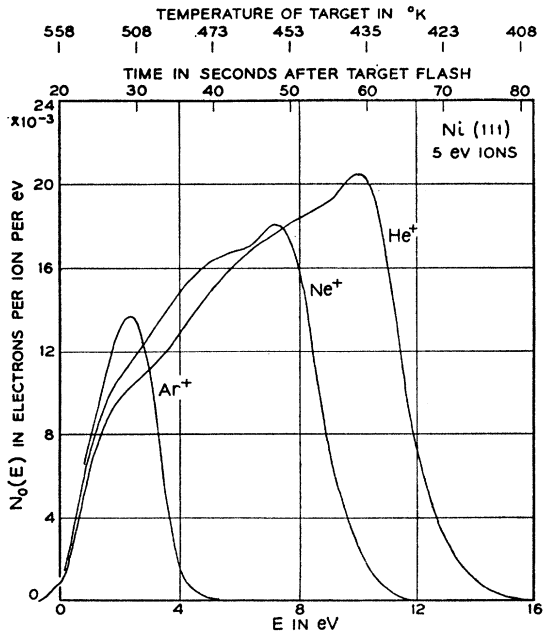


FIG. 2. Kinetic energy distributions  $N_0(E)$  of electrons ejected from the atomically clean (111) face of nickel by He<sup>+</sup>, Ne<sup>+</sup>, and Ar<sup>+</sup> ions of 5-eV incident kinetic energy. At the top, elapsed time after a target flash and corresponding target temperatures are indicated during the period of recording the distributions.

<sup>11</sup> N. Laegreid and G. K. Wehner, J. Appl. Phys. 32, 365 (1961).

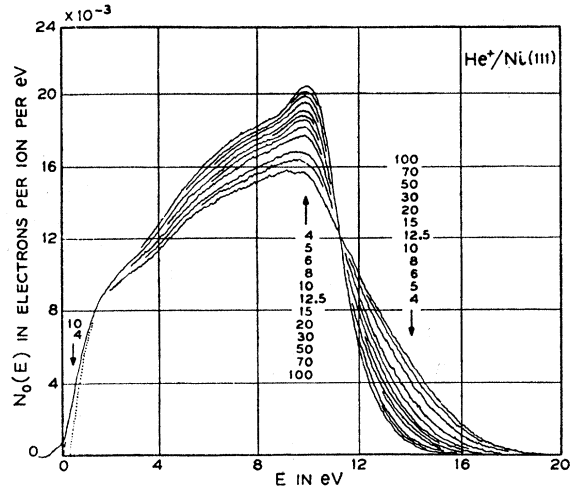


FIG. 3. Variation of the  $N_0(E)$  distribution for He<sup>+</sup> on the clean Ni(111) surface with incident ion kinetic energy  $K$ .  $K$  in eV is indicated in the columns of numbers which correspond in sequence to the curves at the point indicated.

in Fig. 1. The kinetic energy distribution  $N_0(E)$  of electrons ejected from the target is determined as  $d\rho/dV_{ST} = CdI_S/dT$  under the condition of constant ion current and linear change of  $V_{ST}$  with time.  $C$  is a normalization factor determined to yield the measured  $\gamma_i$  by the formula  $\gamma_i = \int_0^\infty N_0(E)dE$ .  $N_0(E)$  was traced directly on an X-Y recorder. The ramp speed of  $V_{ST}$  was 0.26 V/sec in the present measurement. At the top of Fig. 2 is indicated the elapsed time after target flash during the period of recording the  $N_0(E)$  distribution for 5-eV ions. Only 80 sec was needed to complete the run for the case of He<sup>+</sup> which required the longest time, and 65 and 40 sec for 5-eV Ne<sup>+</sup> and Ar<sup>+</sup>, respectively. The temperature change of the target during the run after the target flash is also plotted at the top of Fig. 2. Thus, the target temperature was well above room temperature when the measurements were made. Change in  $\gamma_i$  during the period of 80 sec after the flash was found to be less than 1%. As is discussed later in connection with Fig. 6 we take this to indicate that the elevated temperature of the target prevents adsorption of the residual gases in the apparatus. As shown by dotted lines in Figs. 3 and 4,  $N_0(E)$  for 4-eV ions deviates near  $V_{ST} = 0$  from the other distributions taken at higher ion energies. This is due to focusing failure in this  $V_{ST}$  range for these slow ions. As soon as  $V_{ST}$  is increased by 1 V, however, the focusing is adequate and reasonable results of  $N_0(E)$  were obtained. Thus  $\gamma_i$  measurements are reliable only down to  $K = 5$  eV.

It should be noted that: (1) The kinetic energies of incident ions quoted in this paper are a direct difference in the voltage between the target and the ionization chamber and have not been corrected for the acceleration of the ion toward the target due to image potential (about 1 eV), which is not negligibly small for the slow-

est ions used, and (2) the total energy spread in the ion beams used was about 0.25 eV.

### III. EXPERIMENTAL RESULTS AND DISCUSSION

The values of  $\gamma_i$  obtained for the atomically clean surface of the (111) face of nickel as functions of kinetic energy of incident He<sup>+</sup>, Ne<sup>+</sup>, and Ar<sup>+</sup> ions from 5 to 100 eV are plotted in Fig. 1. In each case,  $\gamma_i$  was observed after the target flash, with the target at a temperature around 560°K as mentioned in the preceding section. We do not expect  $\gamma_i$  at room temperature to be appreciably different. General features of the dependence of  $\gamma_i$  on the incident kinetic energy of He<sup>+</sup>, Ne<sup>+</sup>, and Ar<sup>+</sup> ions are similar to those in the cases of tungsten and molybdenum<sup>2</sup> as well as silicon and germanium,<sup>1</sup> though the general level of the magnitude is relatively lower. In the case of Ne<sup>+</sup> ions, a rapid increase in  $\gamma_i$  with increasing ion energy is indicated and this is probably due to an increasing admixture of two-stage electron ejection relative to the Auger neutralization process, as in the cases of tungsten and molybdenum.<sup>2</sup> The two-stage electron-ejection process is a resonance neutralization of the Ne<sup>+</sup> ion to an excited Ne atom followed by Auger de-excitation.<sup>2</sup>

It should be mentioned that very little reflection of incident ions as ions at the target was observed. This fact is an indication that essentially all of the incident ions are neutralized to atoms by the Auger process.

The kinetic energy distribution  $N_0(E)$  of ejected electrons from the atomically clean surface by 5-eV He<sup>+</sup>, Ne<sup>+</sup>, and Ar<sup>+</sup> ions are given in Fig. 2. These are reproductions of recorder tracings showing the noise inherent in the measurement. The relative forms of these three curves are what we expect if the basic mechanism of the electron ejection is Auger neutralization. The upper energy limits of ejected electrons are approximately the neutralization energy of the ions minus twice the work

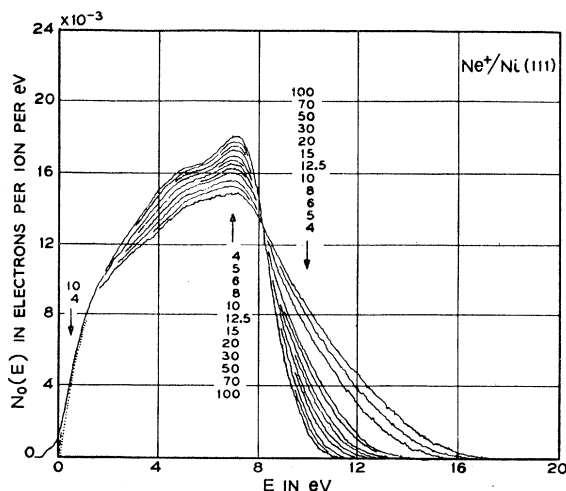


FIG. 4. Variation of the  $N_0(E)$  distribution for Ne<sup>+</sup> on the clean Ni(111) surface with incident ion kinetic energy.

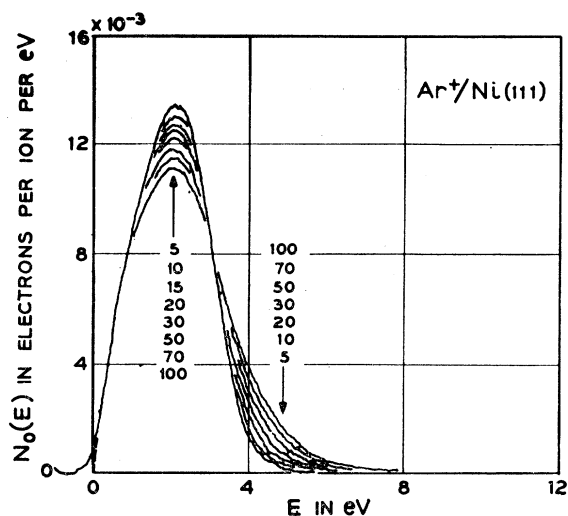


FIG. 5. Variation of the  $N_0(E)$  distribution for Ar<sup>+</sup> on the clean Ni(111) surface with incident ion kinetic energy.

function of the solid and the characteristic features shift on the energy scale with neutralization energy. One can expect from these curves an essentially unique form for the internal distribution of excited electrons in the positive energy continuum produced by the Auger process. Thus, the fact that the form of these electron energy distributions is markedly different from that observed for germanium and silicon indicates a different density of states in the filled band of nickel from that of diamond-type elemental semiconductors, as is expected.

Dependence of  $N_0(E)$  distributions on the kinetic energy of ions has also been measured. The results obtained for He<sup>+</sup>, Ne<sup>+</sup>, and Ar<sup>+</sup> ions in the kinetic energy range 4 to 100 eV are reproduced in Figs. 3, 4, and 5, respectively. Ion kinetic energies which differ by only 1 eV make easily detectable changes in the distributions, particularly for the slower He<sup>+</sup> and Ne<sup>+</sup> ions. Such fine-grained data should make possible detailed investigations into the nature of the inherent physical broadenings of the Auger process. One may also expect to be able to extrapolate these  $N_0(E)$  distributions to obtain essentially unbroadened energy distributions which would be basic data for the extraction of the state density function of nickel. The extension of the tail of the distributions on the energy scale in the case of Ne<sup>+</sup> ion, as ion kinetic energy increases, is larger than that for He<sup>+</sup> ions. This tendency is appreciable for higher energy ions. This fact also suggests an increase in admixture of the Auger de-excitation process to the Auger neutralization process with increasing Ne<sup>+</sup> ion energy, as mentioned above in connection with the  $\gamma_i$  variation with  $K$ . It is interesting to point out that the peak position in  $N_0(E)$  shifts to lower energy by an amount of 0.2 to 0.3 eV as the ion kinetic energy increases from 4 to 100 eV for all three ions. This is taken to indicate

the amount of the decrease in ion neutralization energy as the faster ions are neutralized closer to the solid surface.<sup>1,2</sup>

#### IV. CLEANNES OF TARGET SURFACE AND EFFECT OF GAS ADSORPTION

Cleanness of the target surface in the work described above was carefully examined.  $\gamma_i$  and  $N_0(E)$  taken for the etched surface of the target without any sputtering after evacuation were quite different from the data obtained after sputtering and annealing. As described in Sec. II, several repeated sputterings, each followed by annealing, produced no further change in the data characteristic of the clean surface. As stated, the target was always flashed at about 720°K for 15 sec immediately prior to taking the clean surface data. The data were also shown to be independent of flashing temperature in the range 720 to 1200°K. The target was sputtered when heated (720 to 880°K) producing no change in the data. The target was also heat treated in a hydrogen atmosphere of  $2 \times 10^{-7}$  Torr. Heating at 670°K for 5 min and at 1070°K for 15 sec was repeated three times. It must have completely removed any adsorbed oxygen and/or nickel oxide, if any were present, from the Ni(111) face.<sup>5</sup> Also after this treatment no change appeared in what we call the clean-surface data.

When the target was exposed to residual gases,  $\gamma_i$  and  $N_0(E)$  were greatly affected by adsorption. As an example, a change in  $\gamma_i$  for 10-eV He<sup>+</sup> ion with increasing cold time of the target in residual gases from 15 sec to 24 min after a target flash is plotted in Fig. 6. The background pressure in this case was  $1.5 \times 10^{-9}$  Torr, equivalent nitrogen pressure, which was somewhat higher than that in the work described in the preceding

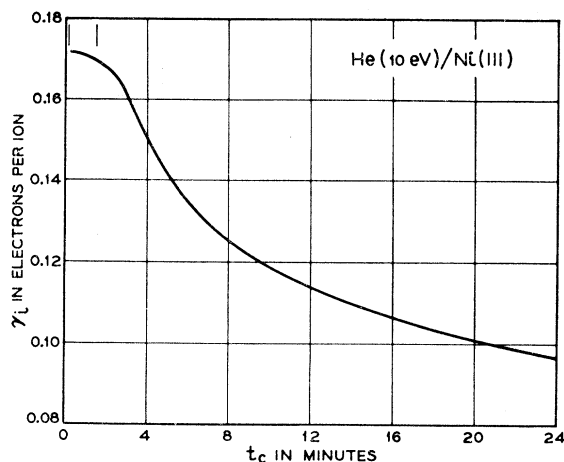


FIG. 6. Variation of total electron yield  $\gamma_i$  for 10-eV He<sup>+</sup> caused by residual gas adsorption as a function of cold time after a target flash. The background pressure was  $1.5 \times 10^{-9}$  Torr. The period from 15 to 80 sec after the target flash, indicated the vertical lines, in which a small decrease in  $\gamma_i$  is seen, corresponds to the time that was needed to record the  $N_0(E)$  distribution.

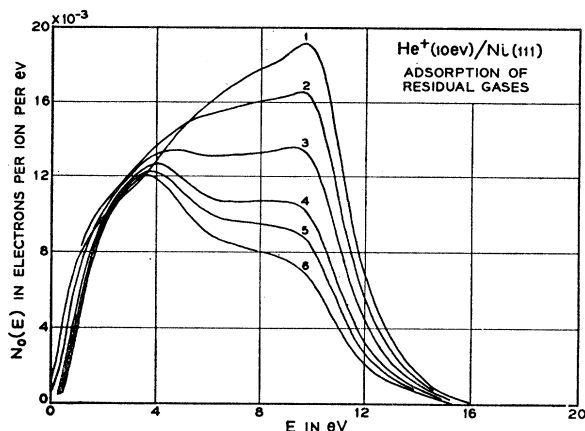


FIG. 7. Change in the  $N_0(E)$  distribution for 10-eV He<sup>+</sup> with the surface coverage by residual gases. Curve 1 was taken 15 sec after the target flash and is identical with the clean surface distribution shown in Fig. 2. Curves 2 and 6 were taken successively 2.5, 4.5, 10, 15, and 25 min after the target flash, respectively. About 80 sec was needed for recording each curve. The area under each curve is approximately equal to the value of  $\gamma_i$  at corresponding time shown in Fig. 6. The scale of electron energy is applicable only to curve 1 as described in the text.

section. The slowness of the initial decrease in  $\gamma_i$  is due to the fact that the target was still well above room temperature (see the top of Fig. 2) so that the surface was kept free from appreciable adsorption. Though no clear level-off of  $\gamma_i$  appears within 24 min, the rate of change tends to decrease. Electron energy distributions for the 10-eV He<sup>+</sup> ion, measured at several points in the adsorption period, are reproduced in Fig. 7. Curves 1 to 6 were those taken at 15 sec, 2.4 min, 4.5 min, 10 min, and 25 min after the target flash, respectively. Curve 1 is what we call the clean-surface distribution. The area under each curve should be approximately equal to the corresponding value of  $\gamma_i$  in Fig. 6. As is seen in Fig. 7, the faster electrons in the clean-surface distribution decreased in number more rapidly with surface coverage than the slow electrons. The electron energy scale applies only to the clean surface distribution. Thus the shift of the low-energy limit in curves 2 to 6 indicates that the work function of the target increased with residual gas adsorption, assuming that the work function of the electron collector remained unchanged. Flashing to 700°K took the distribution from that of curve 6 to the clean surface distribution, curve 1.

Adsorption and removal of O<sub>2</sub>, CO, and H<sub>2</sub> have also been looked at briefly. Recording of  $N_0(E)$  for fractional surface coverage with these gases was not attempted because it was necessary to adsorb them rapidly in order to avoid contamination by the background gases. A large amount of the known gas was quickly admitted into the tube about 1 min after a target flash, and the measurements were made after pumping out the admitted gas. The target temperature during the adsorption was around 400°K. After the target was exposed to

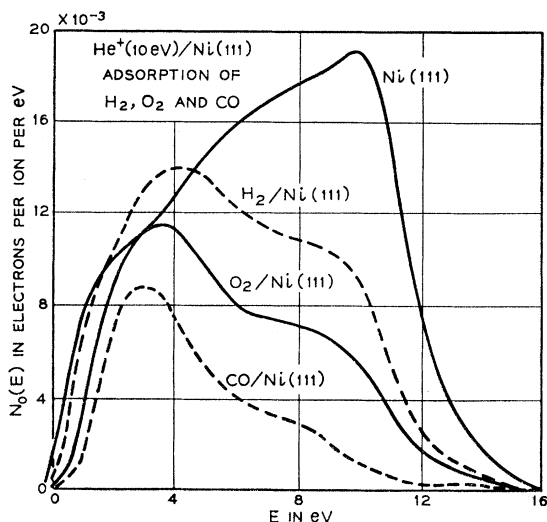


FIG. 8. Relative change in the  $N_0(E)$  distribution for 10-eV  $\text{He}^+$  with adsorption of oxygen, carbon monoxide, and hydrogen. Exposures were  $2.5 \times 10^{-5}$  Torr sec for  $\text{O}_2$ ,  $1.8 \times 10^{-5}$  for CO, and  $2 \times 10^{-4}$  for  $\text{H}_2$ . The clean surface distribution is indicated as Ni(111). The energy scale applies only to the clean surface distribution. Relative change in the contact potential difference between the target and the electron collector as adsorption proceeds is indicated by the relative shift in the low-energy limit of the distributions.

$2.5 \times 10^{-5}$  Torr sec  $\text{O}_2$ ,  $1.8 \times 10^{-5}$  Torr sec CO, and  $2 \times 10^{-4}$  Torr sec  $\text{H}_2$ , the electron energy distributions for 10-eV  $\text{He}^+$  ion were those reproduced in Fig. 8. The sticking probability for  $\text{H}_2$  appears to be much smaller than that for  $\text{O}_2$  and CO. This is consistent with the result of a study by low-energy electron diffraction.<sup>5</sup> The electron energy distributions for the surface covered with these gases resemble those for adsorbed residual gas. The work function of Ni(111) surfaces also appeared to increase with the adsorption of those gases, as is the case for residual gas adsorption, but a careful study of relative shifts of the low-energy and of the  $N_0(E)$  distribution has not been made.

Why the kinetic energy distribution changes as it does with the adsorption of gas is an interesting question. Propst and Lüscher<sup>3</sup> have interpreted the observed change as resulting from the inelastic scattering of the Auger electrons by the adsorbed atoms on the surface. An alternative explanation in terms of wave-function enhancement in what are effectively virtual states of the adsorbed atoms has been presented elsewhere.<sup>12</sup> Our purpose in observing the effects of adsorption in the present work has been to test the reactivity of the target surface as an indication of its cleanliness.

Removal of adsorbed gases on the Ni(111) surface was possible by heating. As an example, thermal regeneration of the "clean" Ni(111) surface after oxygenation is indicated in Fig. 9. Curve 1 is the same as

shown in Fig. 8. Curves 2, 3, and 4 were obtained after successive heating of the target to 380°K for 60 sec, 480°K for 40 sec, and 590°K for 40 sec, respectively. Curve 5 was observed after the last flash to 710°K for 30 sec, and is exactly identical with the clean surface distribution. The distribution did not change from curve 5 on heating to temperatures as high as 1240°K. We note that a change of something less than 1 V in the contact potential between target and electron collector occurs between curves 1 and 2 of Fig. 9 and that no further such change is observed at higher temperatures. This will be discussed further below.

The oxygenated target was also heated in a hydrogen atmosphere by the same process as mentioned above, and the resultant  $N_0(E)$  was exactly the same as curve 5 in Fig. 9. Drastic oxygenation was accomplished by exposing the target held at 700°K to  $3 \times 10^{-4}$  Torr sec of oxygen. The  $N_0(E)$  distribution after this reaction appeared to be something like that between curves 1 and 2 in Fig. 9. For this surface, heating to 720°K for 30 sec was inadequate, but a short flashing to 920°K was adequate to regenerate the clean surface distribution.

Conditions for thermal regeneration of the surface with adsorbed CO and  $\text{H}_2$  as judged from the  $N_0(E)$  distributions were as follows. Carbon monoxide was not completely removed from the surface by heating to 570°K for 60 sec, but 680°K for 20 sec was high enough. For the case of adsorbed hydrogen the clean surface distribution was recovered by a heating to 570°K for 45 sec. Whether any of the adsorbed gases were desorbed into vacuum or diffused into the bulk is not known. In this experiment it is merely possible for us to judge restoration of the Auger distribution which appears to be characteristic of the clean surface.

Sometime after this experiment had been completed

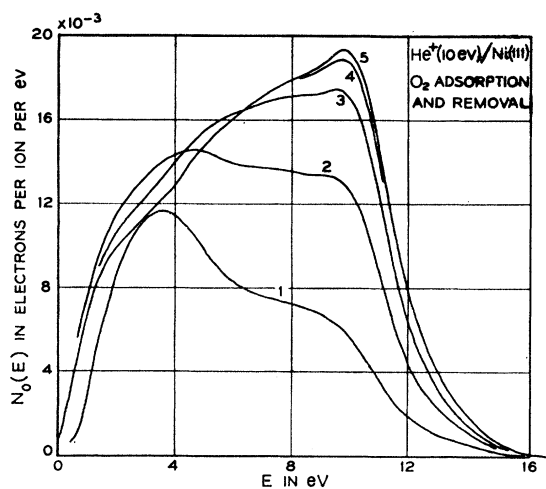


FIG. 9. Thermal restoration of the clean Ni(111) surface after oxygenation. Curve 1 is the  $N_0(E)$  distribution for 10-eV  $\text{He}^+$  incident on the oxygenated surface and is the same as that shown in Fig. 8. Curves 2, 3, 4, and 5 were those obtained after successive heating as explained in the text. Curve 5, observed after heating to 710°K for 30 sec, is identical to the clean surface distribution.

<sup>12</sup> H. D. Hagstrum, Y. Takeishi, G. E. Becker, and D. D. Pretzer, *Surface Science* 2, 26 (1964).

Mac Rae<sup>13</sup> very kindly examined our Ni crystal in his low-energy electron diffraction apparatus. The crystal as removed from the Auger apparatus had a very rough and pitted appearance, possibly due to the heating to 700°K in oxygen for an exposure of  $3 \times 10^{-4}$  Torr sec described above. In this condition Mac Rae was never able to produce the diffraction pattern of a clean, well-ordered Ni(111) surface even after two sputterings by a total of  $10^{18}$  ions each, followed by annealings to 970°K. Complicated patterns, some having the appearance of a (5×5) structure, others involving NiO spots, were obtained. The crystal was then removed from the diffraction apparatus and etched in the same manner as had been done before insertion into the Auger tube. The crystal was now bright and smooth. After vacuum processing and heating to 650°K only it exhibited a good  $(\sqrt{3} \times \sqrt{3})R(30^\circ)$  pattern. The target was sputtered and annealed, and exposed to oxygen after which only a weak (2×2) structure was observed. The clean pattern could be restored by heating to 1070°K. After a second sputter and anneal, and two oxygen admissions and clean surface regenerations by heating, a good, strong (2×2) pattern was obtained on exposure to  $\sim 1 \times 10^{-6}$  Torr sec of oxygen as Mac Rae had found previously.<sup>5</sup> It was then possible to remove the (2×2) structure at a temperature of approximately 770°K, the lowest observed by Mac Rae in experimentation with several crystals. The work function increase from the clean surface to the (2×2) structure was then measured by Mac Rae for this crystal as 1.3 eV and an additional 0.8-eV increase was observed in going from the (2×2) structure to the "transition" structure involving weak  $(\sqrt{3} \times \sqrt{3})R(30^\circ)$  spots obtained by further oxygenation. Both of these results agree with Mac Rae's earlier work. Park and Farnsworth<sup>14</sup> report that heating to 1120°K did not decompose their Ni<sub>3</sub>O film and that the photoelectric work function with this film on the surface was 0.2 eV higher than that of the clean (111) surface.

There remains the problem of correlating these various results. The following statements can be made: The repeated sputterings and annealings during the Auger experiment, which resulted in a reproducible "clean-surface" kinetic energy distribution, is believed to characterize a surface which has very little impurity on it adsorbed from the gas phase. This surface is also reactive to O<sub>2</sub>, H<sub>2</sub>, CO and the residual gases in the apparatus. It has not been demonstrated, however, that this surface did not have an impurity, whose source was the bulk crystal and which diffused onto the surface during the annealing period. This is felt to be unlikely

because of the reproducibility and of the experiment and the various annealing temperatures used, and also because the crystal in Mac Rae's subsequent experiments could eventually be restored to its clean conditions, as judged by the diffraction patterns, and could then withstand heating to high temperatures without pattern degeneration. However, in the condition in which the target was removed from the Auger experiment this was not the case, as pointed out above, even though the "clean" Auger characteristic had been obtained with the crystal presumably in this condition. We do not understand this last result.

The temperature (710°K) required to restore the clean-surface Auger distribution, Fig. 9, whereas it is somewhat lower than the lowest ( $\sim 770^\circ\text{K}$ ) observed by Mac Rae, is not considered unreasonable in view of the wide range of temperatures observed earlier by Mac Rae and our own observation that a drastically oxygenated surface had to be heated to 920°K for regeneration of the clean Auger characteristics. Both this work and Mac Rae's show that the temperature to remove oxygen is strongly dependent on the previous history of the sample, apparently becoming greater with increasing amounts of oxygen dissolved in the bulk crystal.

A more serious discrepancy between the present results and those of Mac Rae concerns work function changes. To the extent that the contact potential shifts of the low-energy end of the  $N_0(E)$  distribution can be taken as work function changes of the nickel target, the data of Fig. 9 indicate a work function increase of something less than 1 eV. This increase disappears on heating to 380°K for 60 sec since the low-energy position of  $N_0(E)$  is then seen to shift back to a position which is unchanged on further heating. Correlation with Mac Rae's work would say that this corresponds to the 0.8 eV work-function change observed in going from the (2×2) structure to the "intermediate" structure. However, there is no evidence in this work of the 1.3 eV work-function change from the (2×2) structure to the clean surface observed by Mac Rae in the diffraction apparatus. Park and Farnsworth's work-function measurements also indicate smaller work-function changes. It is hoped that a resolution of these differences will be possible with a new apparatus in which both Auger and low-energy electron diffraction experiments can be conducted in the same vacuum on the same sample.

#### ACKNOWLEDGMENTS

It is a pleasure to acknowledge many helpful discussions with Dr. A. U. Mac Rae, and to thank him for his study of our crystal after these experiments. We are also grateful to C. D'Amico for technical assistance during the experimentation.

<sup>13</sup> A. U. Mac Rae (private communication).

<sup>14</sup> R. L. Park and H. E. Farnsworth, Appl. Phys. Letters 3, 167 (1963).